Article

Species intraspecific variation drives tropical forest drought resistance

https://doi.org/10.1038/s41586-026-10870-4

Received: 25 May 2025

Accepted: 1 July 2026

Published online: 12 August 2026

Check for updates

Chris M. Smith-Martin[1,2]✉, Robert Muscarella[3], Timothy J. Brodribb[4] & María Uriarte[2]

Severe droughts are increasingly driving tree mortality, yet predicting forest resilience remains limited by a lack of understanding of within-species variation in drought resistance[1–4]. Although hydraulic traits such as embolism resistance are central to drought survival, studies conducted primarily in temperate regions have reported little intraspecific variation[5–12], implying that there are evolutionary constraints in the adaptive potential of tree species. Here we test this assumption using a dataset comprising 11 hydraulic traits for 290 trees representing 18 species collected along Puerto Rico's fourfold rainfall gradient (1,000 to 4,000 mm per year). We find that substantial intraspecific variation, together with species turnover, drives coordinated shifts in drought resistance across the gradient. Most species exhibit substantially more embolism resistance and wider stomatal safety margins in drier forests, demonstrating a considerable level of intraspecific variation in tropical trees and a mechanism for adaptation to increasingly dry conditions. Species lacking such trait variability may be highly vulnerable under a future drier climate. Incorporating both interspecific and intraspecific trait variation into predictive models will advance our ability to forecast forest resilience to intensifying droughts.

Severe droughts have led to widespread tree mortality and growth declines across tropical forests[1–4]. As these ecosystems account for the majority of terrestrial aboveground biomass[13], elevated tree mortality could lead to large carbon losses to the atmosphere, transforming these forests from a carbon sink to a source and exacerbating climate warming[14]. As drought events are anticipated to intensify and lengthen[15], high mortality rates are likely to persist and even rise[16]. However, drought impacts differ among tropical tree species, populations and communities[4]. These differences may lead to shifts in species composition and species geographic ranges[17,18]. On the other hand, tree species may have enough intraspecific variation in drought resistance to withstand severe droughts. The capacity of tropical forests to mitigate climate change hinges on the capacity of tree species and communities to survive changing precipitation patterns[19].

Understanding the extent of both interspecific and intraspecific variation in drought resistance, including traits related to drought tolerance and drought avoidance, is essential for predicting tropical forest responses to climate change. Previous studies show that co-occurring tropical tree species differ widely in their resistance to drought[4,20,21], influencing species abundance and distribution[22–24]. While interspecific variation has been more thoroughly studied, intraspecific variation, particularly in hydraulic traits directly linked to physiological function, remains poorly understood. Many tropical tree species span broad rainfall gradients[24,25], yet intraspecific variation in hydraulic traits has rarely been examined across multiple species. Most work on intraspecific variation in hydraulic traits, such as xylem vulnerability to embolism, comes from temperate and Mediterranean regions, where studies generally report no adjustment to climatic water availability[5,7,8,26,27]. The few studies that have focused on tropical systems have measured only one or two species at a small spatial scale, limiting our ability to draw inferences at broader taxonomic and climate scales[25,28]. Tropical studies with larger numbers of species have focused on morphological traits (such as specific leaf area and wood density) as proxies for physiological functions[19], but these traits often fail to predict which species experience growth declines or mortality during severe droughts[4]. These limitations highlight the need for multispecies datasets on interspecific and intraspecific variation in hydraulic traits for predicting tropical forest responses to drought and constraining forecasts of changes in species composition, range shifts and ecosystem resilience under future climate scenarios[19,29,30].

To fill this knowledge gap, we studied tropical forests along a steep rainfall gradient (1,000–4,000 mm per year) in Puerto Rico. This island-wide system provides an ideal setting to evaluate the relative contribution of intraspecific variation and species turnover to forest drought resistance. We measured 11 plant hydraulic traits for 18 tree species in 6 different forest reserves spanning the island's rainfall gradient. Together, these species account for 18–75% of tree stems (≥5 cm diameter) depending on the site (Fig. 1, Extended Data Fig. 1, Extended Data Tables 1 and 2 and Supplementary Table 1). We included traits linked to drought avoidance, such as leaf and stem capacitance, saturated water content (SWC) and drought tolerance, such as leaf and stem xylem vulnerability to embolism (stem xylem water potential at 50% embolism accumulation (P_{50})) and stomatal safety margins (SMP_{50} = turgor loss point (TLP) − P_{50}). Traits were measured in as many of the 6 sites as each

[1]Department of Plant and Microbial Biology, University of Minnesota, Saint Paul, MN, USA. [2]Department of Ecology Evolution and Environmental Biology, Columbia University, New York, NY, USA. [3]Plant Ecology and Evolution, Evolutionary Biology Centre, Uppsala University, Uppsala, Sweden. [4]ARC Centre of Excellence for Plant Success in Nature and Agriculture, School of Natural Sciences, University of Tasmania, Hobart, Tasmania, Australia. ✉e-mail: smithmar@umn.edu

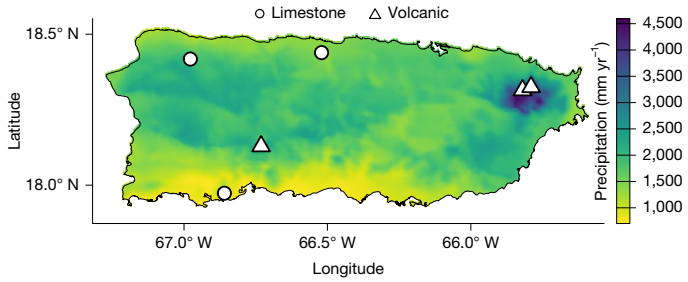

Fig. 1 | Island-wide precipitation gradient and study sites. Map of the island of Puerto Rico coloured by the gradient of MAP. The locations of the six study sites are shown as circles (limestone soils) or triangles (volcanic soils). Further details were reported previously[36,49].

species occurred, totalling 290 trees, with all species measured at 2–4 locations (Supplementary Table 2). Using this dataset, we examined (1) how hydraulic traits associated with different drought resistance strategies (that is, drought avoidance and drought tolerance) shifted across the island's steep rainfall gradient; and (2) the relative contribution of intraspecific variation versus species turnover to these shifts. This study represents a comprehensive assessment of intraspecific variation in hydraulic traits for tropical forest trees.

Drought avoidance and tolerance

Across the rainfall gradient, we observed a shift in dominant drought resistance strategies: trees at drier sites exhibited trait values associated with greater drought tolerance, while those at wetter sites displayed trait values associated with more pronounced drought avoidance. Species-level trait means revealed that drier forest sites had higher resistance to embolism and stomatal safety margins in both leaves and stems (Fig. 2a,b,d,e), whereas wetter sites had higher average leaf and stem capacitance, and greater stem SWC (Fig. 2h–k). There was no association between leaf TLP and rainfall (Fig. 2c), indicating that the observed association between stomatal safety margins and rainfall was driven by variation in P_{50} rather than TLP. There was no association between leaf saturated water content (Fig. 2f) and leaf capacitance at full turgor (Fig. 2g) and rainfall. Overall, our findings suggest that drought tolerance strategies are more successful in forests subject to prolonged and intense water stress, while drought avoidance traits are more common in wetter forests where water shortages are shorter and less severe. These patterns are consistent with previous work in temperate precipitation gradients in Australia, where species showed increasing drought tolerance (P_{50} and SMP_{50}) with decreasing rainfall[31,32]. Our findings show that this pattern is also true for diverse tropical forests and offer a new dimension: drought avoidance traits also shift along rainfall gradients, increasing with higher rainfall.

The positive relationship between site-level drought tolerance and decreasing rainfall was stronger than the corresponding decrease in drought avoidance (Fig. 3 and Supplementary Tables 3 and 4). When accounting for intraspecific variation, most traits related to drought tolerance exhibited significant shifts across the rainfall gradient (Fig. 3a,b,d,e and Supplementary Tables 3 and 4), while most drought-avoidance traits did not (Fig. 3h–k and Supplementary Tables 3 and 4). This asymmetry may be partly explained by the difference in soil type and moisture retention. All three wetter sites, where drought avoidance dominates, have volcanic soil that retain moisture well[33–35] and share relatively high mean rainfall (2,195–4,029 mm; Extended Data Table 1) and weak seasonality[36]. As a result, trees at these sites probably experience similarly low levels of drought stress, contributing to comparable drought avoidance trait values. By contrast, the three drier sites at which drought tolerance is more prevalent all share limestone soil with poor water retention[33–35]. These sites also experience higher vapour pressure deficit (Extended Data Table 1) and lower rainfall (mean annual precipitation (MAP) = 1,004–2,017 mm), probably leading to greater variability in drought stress and stronger trait–environment associations[33–35]. As soil type and rainfall are confounded in our study, all the wetter sites have volcanic-derived soil and all the drier sites have limestone-derived soil, we cannot fully disentangle their effects. However, the confounding of rainfall and soil type is inherent to the island's landscape and does not negate the biological signal.

Species turnover and intraspecific variation

Site-level drought resistance traits varied substantially across the precipitation gradient. For example, site-average leaf P_{50} ranged from −2.74 to −5.79 and leaf stomatal safety margins from 0.95 to 3.82 MPa among sites, reflecting a combination of species turnover and intraspecific trait variation (Supplementary Table 5). On average, species turnover accounted for 39% of the variance in hydraulic traits across sites, ranging from 18% for leaf capacitance at TLP (CTLP) to 66% for leaf SWC (Supplementary Table 6). Intraspecific variation explained a smaller, yet significant, proportion of variance, averaging 13% across all traits, with values ranging from 1% for leaf SWC to 23% for stem capacitance at full turgor (CFT). Notably, leaf P_{50} and leaf SMP_{50} each showed 17% intraspecific contribution to the observed variation, which is substantial (Fig. 4 and Supplementary Table 6). Note that, owing to our sampling scheme, which focused on species that occurred at more than one of the six plots, we measured only a subset of species within each plot (Extended Data Fig. 1).

In analyses conducted at the individual species level, 17 out of the 18 study species exhibited statistically significant intraspecific variation across the rainfall gradient for at least 1 of the 11 hydraulic traits measured (Supplementary Tables 7 and 8). The number of traits with statistically significant levels of intraspecific variation per species ranged from one to ten (Supplementary Tables 7 and 8). Species with statistically significant intraspecific variation generally mirrored site-level trends, with increasing drought tolerance in drier sites (Fig. 3a,b,d,e and Supplementary Tables 7 and 8) and higher drought avoidance in wetter sites (Fig. 3h–k and Supplementary Tables 7 and 8). However, different species exhibited intraspecific variation in different combinations of traits and magnitudes. Traits most frequently exhibiting intraspecific variation included leaf P_{50}, stem P_{50}, leaf SMP_{50}, stem SMP_{50}, leaf CFT, stem SWC, stem CFT and stem CTLP (Supplementary Tables 7 and 8). These traits are associated with embolism resistance, hydraulic safety and stem water storage, highlighting their central role in drought resistance across the island. Although studies have found limited intraspecific variation in morphological traits of tropical seedlings[19], our findings reveal substantial variation in hydraulic traits among adult trees. This difference suggests that local water availability may exert stronger selective pressure on hydraulic traits[21] than on morphological traits and stronger selective pressure on adult trees rather than seedlings.

Previous studies of intraspecific variation in hydraulic traits of tropical trees have been limited and have yielded mixed results. For example, one study[25] found substantial differences in P_{50} between wet and dry sites for *Cordia alliodora* (MAP = 4,200 mm and P_{50} = −1.78 (wet), and MAP = 1,460 mm and P_{50} = −3.60 (dry)), consistent with our findings for many more species spanning a broader rainfall gradient. By contrast, a study comparing two dominant Amazonian tree species across water table depths found increased embolism resistance in the drier site for only one species[28]. Similarly, a long-term throughfall exclusion experiment in the Amazon[37] documented substantial osmotic adjustment in response to the imposed long-term drought but focused on a limited number of species at a single site, precluding extrapolation to a larger number of species across marked rainfall gradients. Collectively, these studies suggest that tropical trees may exhibit intraspecific variation in hydraulic traits in response to water availability, but their limited taxonomic scope and spatial extent have precluded broader generalization across marked rainfall gradients.

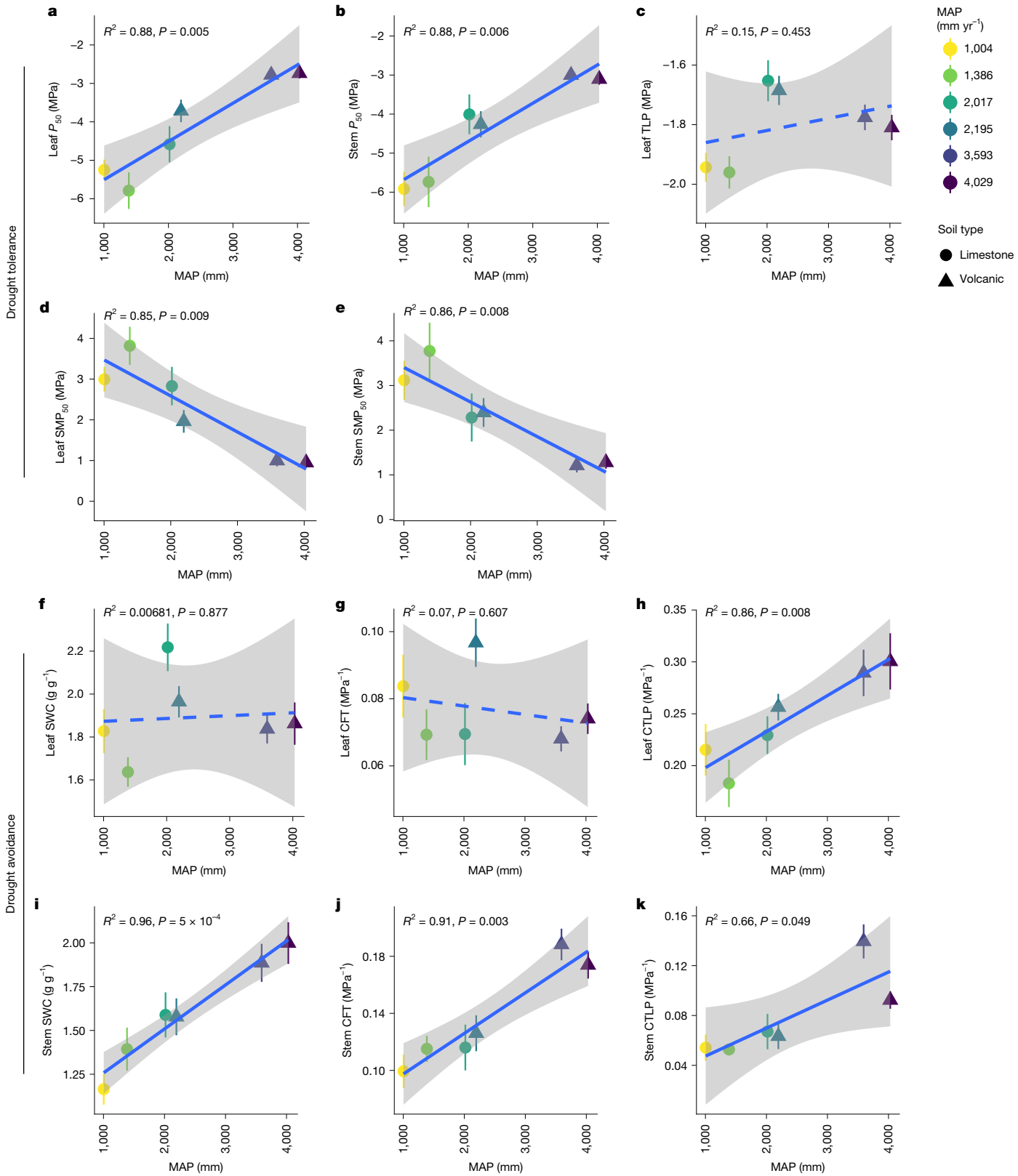

Fig. 2 | Association between MAP and hydraulic traits. a–k, Association between MAP and the site-level species means of leaf P_{50} (**a**); stem P_{50} (**b**); leaf TLP (**c**); leaf (**d**) and stem (**e**) stomatal safety margins (SMP_{50} = TLP − P_{50}); leaf SWC (**f**); leaf CFT (**g**); leaf CTLP (**h**); stem SWC (**i**); stem CFT (**j**); and stem CTLP (**k**). The blue lines show the results of linear regressions and the shaded areas indicate the 95% confidence intervals. Data are mean ± s.e.m. Colours indicate each of the six sites where the measurements were conducted, and their respective MAP; the symbols indicate the soil type. n = 290 measured trees from 18 tree species.

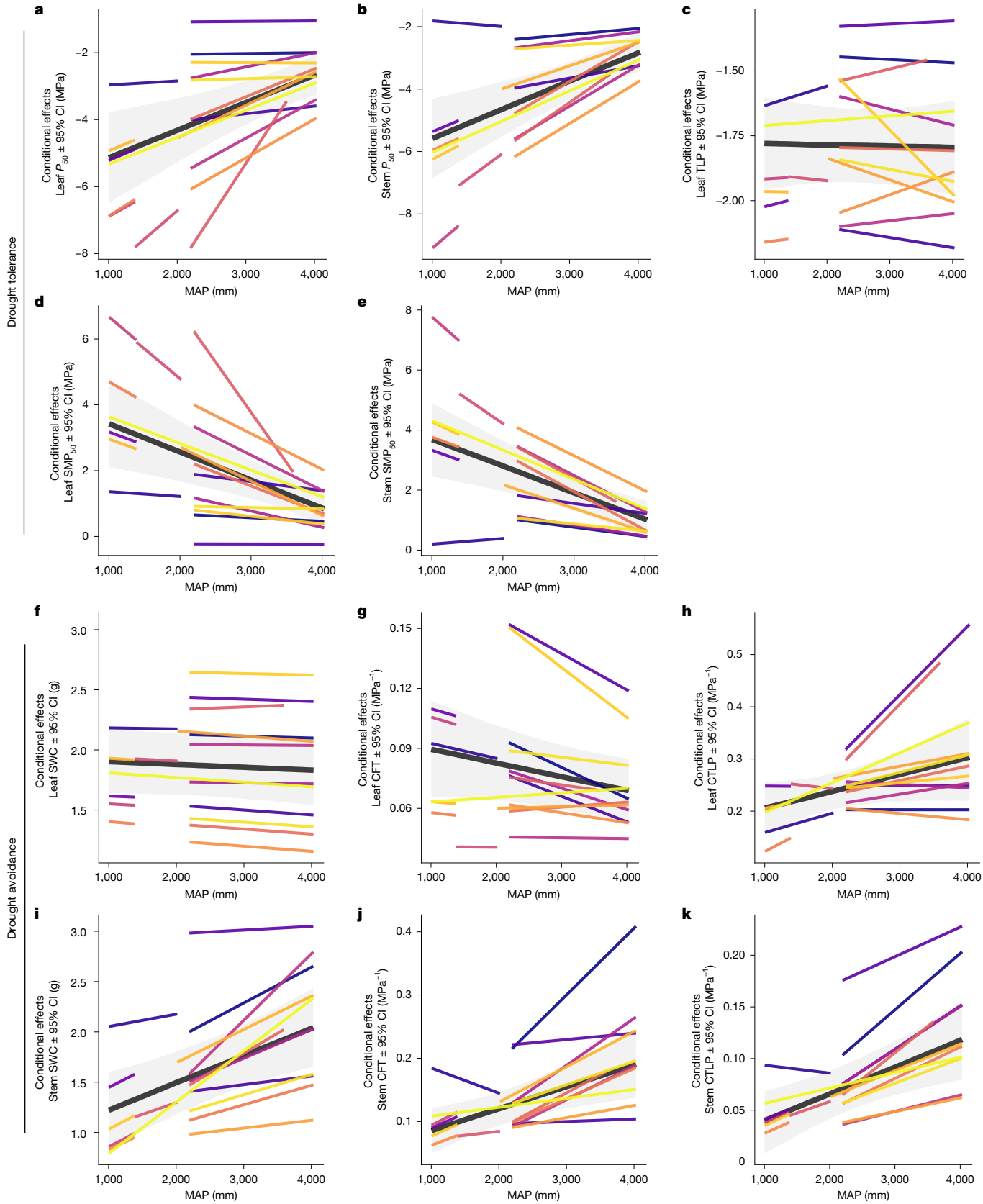

Fig. 3 | Conditional effects of hydraulic traits by MAP. a–k, The solid black lines depict the overall conditional effects from the Bayesian hierarchical models of leaf P_{50} (**a**); stem P_{50} (**b**); leaf TLP (**c**); leaf (**d**) and stem (**e**) SMP_{50}; leaf SWC (**f**); leaf CFT (**g**); leaf CTLP (**h**); stem SWC (**i**); stem CFT (**j**); and stem CTLP (**k**) and scaled MAP. The shaded areas are the 95% credible intervals (CIs). The coloured lines show the species-specific posterior predictions for random slope effects from the Bayesian hierarchical models for each hydraulic trait restricted to the sites where they occurred. Note that the hydraulic trait responses to the rainfall gradient are not the same across species, so colours represent different species among panels (details on species-level intraspecific variation are provided in Supplementary Tables 7 and 8). $n = 290$ measured trees from 18 tree species.

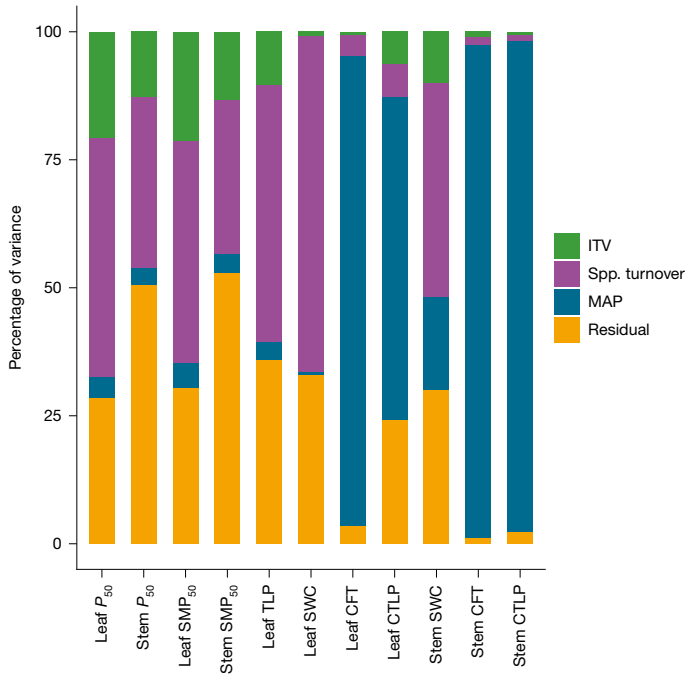

Fig. 4 | Variance partition. The percentage of variance from each of the Bayesian hierarchical models for each of the hydraulic traits that are explained by the random slopes of the models (intraspecific trait variation, ITV), the random intercepts of the models (species (Spp.) turnover), the fixed effect of MAP and the residual unexplained variance. The traits are leaf P_{50} and stem P_{50}, leaf and stem SMP_{50}, leaf TLP, leaf SWC, leaf CFT, leaf CTLP, stem SWC, stem CFT and stem CTLP. $n = 290$ measured trees from 18 tree species.

As empirical evidence from tropical forests remains limited, much of our current understanding of intraspecific variation in hydraulic traits derives from studies conducted in temperate and Mediterranean ecosystems. Across these systems, research on P_{50} and related hydraulic traits in both conifers and angiosperms report limited within-species variability or weak adaptive differentiation across aridity gradients, patterns often interpreted as evidence of strong genetic canalization under stabilizing selection[5–12]. Instead, drought responses in these regions are thought to occur primarily through variation in allocation strategies (for example, leaf:sapwood ratios) and plasticity or adaptation in traits such as leaf mass per area, wood density and Huber values, rather than through changes in intrinsic xylem vulnerability to embolism[5–8,38–40]. This body of work has contributed to a prevailing view that hydraulic traits are largely conserved within species, particularly in environments characterized by strong seasonality and repeated drought exposure. Against this backdrop, our results highlight a marked departure from the prevailing paradigm derived largely from temperate systems. We find that most tropical tree species exhibit greater xylem resistance to embolism (that is, more negative P_{50} values) and larger stomatal safety margins at drier sites, indicating substantial intraspecific variation in hydraulic traits across rainfall gradients. These patterns suggest that tropical tree species may possess greater hydraulic flexibility than their temperate counterparts, with intrinsic xylem properties varying in response to long-term differences in water availability. Such flexibility has important implications for predicting drought vulnerability in tropical forests, a biome that has a disproportionate role in global biodiversity and climate regulation, underscoring the need to explicitly incorporate intraspecific hydraulic variation into process-based vegetation models. In tropical wet forests, complex biogeographical histories[41,42] combined with relatively weak and spatially heterogeneous climatic filtering may promote the maintenance of this variation within species. Understanding the origins, limits and consequences of such variation represents an important frontier for improving predictions of tropical forest responses to intensifying drought under climate change.

The mechanisms generating observed intraspecific phenotypic variation in hydraulic traits probably include genetic differentiation, phenotypic plasticity and transgenerational environmental effects. Evidence from temperate and semi-arid systems shows that populations adapted to distinct rainfall regimes diverge in hydraulic and water use traits while retaining strong plasticity to short-term drought[43–45]. Moreover, maternal environments can influence physiological performance in subsequent generations. For example, the offspring of *Eucalyptus grandis* trees from wetter origins exhibit higher growth and water use efficiency[46], suggesting that epigenetic inheritance may contribute to drought acclimation. A recent global meta-analysis, based largely on temperate species, found plastic adjustments in hydraulic traits under drier conditions, including increases in embolism resistance and sapwood per leaf area, and decreases in stem-specific hydraulic conductivity and leaf TLP[47]. However, these adjustments were insufficient to offset declines in plant water potential, resulting in reduced hydraulic safety margins under drought[47]. Such interactions among adaptation, plasticity and transgenerational effects imply that intraspecific trait variation in tropical trees could reflect both evolutionary divergence and environmental memory, enhancing species' ability to persist under non-stationary climates. Another possible explanation is that although drought occurs in both temperate and tropical environments, the nature of environmental filtering differs. In temperate and Mediterranean regions, recurrent and relatively predictable seasonal stresses—including drought and, in many systems, freezing—may impose strong stabilizing selection on hydraulic traits. In particular, temperature-related constraints on xylem structure associated with freezing risk are known to limit variation in conduit architecture and embolism resistance[48]. By contrast, tropical forests experience relatively uniform temperatures and often more irregular drought regimes, which may weaken consistent selective pressures and allow greater phenotypic variation in hydraulic traits to be maintained within species. Future studies combining physiological, genomic and experimental approaches will be crucial to disentangle the relative contributions of these mechanisms to drought resistance in tropical forests.

Conclusion

By measuring hydraulic traits for a large number of tropical tree species across a steep rainfall gradient, we found that 17 out of 18 species exhibited significant directional shifts in hydraulic trait values, indicating that phenotypes can adjust in response to local water availability. Species exhibiting intraspecific variation in drought-related traits may be better equipped to cope with future climate scenarios with more frequent and intense droughts. By contrast, species lacking such variability may be less able to adapt, potentially leading to shifts in species geographical distributions and forest composition that favour those with greater trait phenotypic variation. Across both the site level and species level, drought-tolerant traits were more common in drier environments, while drought-avoidant traits predominated in wetter sites. The widespread occurrence of intraspecific variation in hydraulic traits suggests that tropical forests may possess greater adaptive capacity to changing rainfall regimes than previously recognized. This phenotypic variation could have a critical role in buffering forest function and maintaining biodiversity under climate change.

Online content

Any methods, additional references, Nature Portfolio reporting summaries, source data, extended data, supplementary information, acknowledgements, peer review information; details of author contributions and competing interests; and statements of data and code availability are available at https://doi.org/10.1038/s41586-026-10870-4.

1. Aleixo, I. et al. Amazonian rainforest tree mortality driven by climate and functional traits. *Nat. Clim. Change* **9**, 384–388 (2019).
2. Uriarte, M., Lasky, J. R., Boukili, V. K. & Chazdon, R. L. A trait-mediated, neighbourhood approach to quantify climate impacts on successional dynamics of tropical rainforests. *Funct. Ecol.* **30**, 157–167 (2016).
3. Leitold, V. et al. El Niño drought increased canopy turnover in Amazon forests. *N. Phytol.* **219**, 959–971 (2018).
4. Powers, J. S. et al. A catastrophic tropical drought kills hydraulically vulnerable tree species. *Glob. Change Biol.* **26**, 3122–3133 (2020).
5. Rosas, T. et al. Adjustments and coordination of hydraulic, leaf and stem traits along a water availability gradient. *N. Phytol.* **223**, 632–646 (2019).
6. Anderegg, L. D. L. et al. Aridity drives coordinated trait shifts but not decreased trait variance across the geographic range of eight Australian trees. *N. Phytol.* **229**, 1375–1387 (2021).
7. López, R., Cano, F. J., Martin-StPaul, N. K., Cochard, H. & Choat, B. Coordination of stem and leaf traits define different strategies to regulate water loss and tolerance ranges to aridity. *N. Phytol.* **230**, 497–509 (2021).
8. Alon, A. et al. Acclimation limits for embolism resistance and osmotic adjustment accompany the geographical dry edge of Mediterranean species. *Funct. Ecol.* **37**, 1421–1435 (2023).
9. Maherali, H., Williams, B. L., Paige, K. N. & Delucia, E. H. Hydraulic differentiation of Ponderosa pine populations along a climate gradient is not associated with ecotypic divergence. *Funct. Ecol.* **16**, 510–521 (2002).
10. Martínez-Vilalta, J. et al. Hydraulic adjustment of Scots pine across Europe. *N. Phytol.* **184**, 353–364 (2009).
11. Lamy, J. B. et al. Limited genetic variability and phenotypic plasticity detected for cavitation resistance in a Mediterranean pine. *N. Phytol.* **201**, 874–886 (2014).
12. Sáenz-Romero, C. et al. Genetic variation of drought-induced cavitation resistance among *Pinus hartwegii* populations from an altitudinal gradient. *Acta Physiol. Plant.* **35**, 2905–2913 (2013).
13. Pan, Y. et al. A large and persistent carbon sink in the world's forests. *Science* **333**, 988–993 (2011).
14. Gatti, L. V. et al. Drought sensitivity of Amazonian carbon balance revealed by atmospheric measurements. *Nature* **506**, 76–80 (2014).
15. Seo, K.-W. et al. Abrupt sea level rise and Earth's gradual pole shift reveal permanent hydrological regime changes in the 21st century. *Science* **387**, 1408–1413 (2025).
16. Brodribb, T. J., Powers, J., Cochard, H. & Choat, B. Hanging by a thread? Forests and drought. *Science* **368**, 261–266 (2020).
17. Fauset, S. et al. Drought-induced shifts in the floristic and functional composition of tropical forests in Ghana. *Ecol. Lett.* **15**, 1120–1129 (2012).
18. Trugman, A. T., Anderegg, L. D. L., Shaw, J. D. & Anderegg, W. R. L. Trait velocities reveal that mortality has driven widespread coordinated shifts in forest hydraulic trait composition. *Proc. Natl Acad. Sci. USA* **17**, 8532–8538 (2020).
19. Comita, L. S. et al. Limited intraspecific variation in drought resistance along a pronounced tropical rainfall gradient. *Proc. Natl Acad. Sci. USA* **121**, e2316971121 (2024).
20. Smith-Martin, C. M. et al. Hydraulic variability of tropical forests is largely independent of water availability. *Ecol. Lett.* **26**, 1829–1839 (2023).
21. Vargas G, G. et al. Leaf habit affects the distribution of drought sensitivity but not water transport efficiency in the tropics. *Ecol. Lett.* **25**, 2637–2650 (2022).
22. Tavares, J. V. et al. Basin-wide variation in tree hydraulic safety margins predicts the carbon balance of Amazon forests. *Nature* **617**, 111–117 (2023).
23. Engelbrecht, B. M. J. et al. Drought sensitivity shapes species distribution patterns in tropical forests. *Nature* **447**, 80–82 (2007).
24. Esquivel-Muelbert, A. et al. Seasonal drought limits tree species across the Neotropics. *Ecography* **40**, 618–629 (2017).
25. Choat, B., Sack, L. & Holbrook, N. M. Diversity of hydraulic traits in nine *Cordia* species growing in tropical forests with contrasting precipitation. *N. Phytol.* **175**, 686–698 (2007).
26. Westerband, A. C., Funk, J. L. & Barton, K. E. Intraspecific trait variation in plants: a renewed focus on its role in ecological processes. *Ann. Bot.* **127**, 397–410 (2021).
27. Tonet, V., Brodribb, T. & Bourbia, I. Variation in xylem vulnerability to cavitation shapes the photosynthetic legacy of drought. *Plant Cell Environ.* **47**, 1160–1170 (2024).
28. Garcia, M. N. et al. Local hydrological gradients structure high intraspecific variability in plant hydraulic traits in two dominant central Amazonian tree species. *J. Exp. Bot.* **73**, 939–952 (2022).
29. Benito Garzón, M., Alía, R., Robson, T. M. & Zavala, M. A. Intra-specific variability and plasticity influence potential tree species distributions under climate change. *Glob. Ecol. Biogeogr.* **20**, 766–778 (2011).
30. Valladares, F. et al. The effects of phenotypic plasticity and local adaptation on forecasts of species range shifts under climate change. *Ecol. Lett.* **17**, 1351–1364 (2014).
31. Blackman, C. J. et al. Leaf hydraulic vulnerability to drought is linked to site water availability across a broad range of species and climates. *Ann. Bot.* **114**, 435–440 (2014).
32. Peters, J. M. R. et al. Living on the edge: a continental-scale assessment of forest vulnerability to drought. *Glob. Change Biol.* **27**, 3620–3641 (2021).
33. Daly, C., Helmer, E. H. & Quiñones, M. Mapping the climate of Puerto Rico, Vieques and Culebra. *Int. J. Climatol.* **23**, 1359–1381 (2003).
34. Miller, G. & Lugo, A. E. *Guide to the Ecological Systems of Puerto Rico* (US Department of Agriculture, 2009).
35. US Geological Survey Minerals Team. *Geology, Geochemistry, Geophysics, Mineral Occurrences, and Mineral Resource Assessment for the Commonwealth of Puerto Rico* Open-File Report 98-38 (US Geological Survey, 1998).
36. Muscarella, R., Kolyaie, S., Morton, D. C., Zimmerman, J. K. & Uriarte, M. Effects of topography on tropical forest structure depend on climate context. *J. Ecol.* **108**, 145–159 (2020).
37. Binks, O. et al. Plasticity in leaf-level water relations of tropical rainforest trees in response to experimental drought. *N. Phytol.* **211**, 477–488 (2016).
38. Schuldt, B. et al. How adaptable is the hydraulic system of European beech in the face of climate change-related precipitation reduction? *N. Phytol.* **210**, 443–458 (2016).
39. Hajek, P., Kurjak, D., Von Wühlisch, G., Delzon, S. & Schuldt, B. Intraspecific variation in wood anatomical, hydraulic, and foliar traits in ten European beech provenances differing in growth yield. *Front. Plant Sci.* **7**, 791 (2016).
40. Skelton, R. P. et al. Evolutionary relationships between drought-related traits and climate shape large hydraulic safety margins in western North American oaks. *Proc. Natl Acad. Sci. USA* **118**, e2008987118 (2021).
41. Dick, C. W. & Pennington, R. T. History and geography of neotropical tree diversity. *Ann. Rev. Ecol. Evol. Syst.* **50**, 279–301 (2019).
42. Baker, P. A. et al. in *Neotropical Diversification: Patterns and Processes* (eds Rull, V. & Carnaval, A. C.) 51–70 (Springer, 2020).
43. Knutzen, F., Meier, I. C. & Leuschner, C. Does reduced precipitation trigger physiological and morphological drought adaptations in European beech (*Fagus sylvatica* L.)? Comparing provenances across a precipitation gradient. *Tree Physiol.* **35**, 949–963 (2015).
44. McLean, E. H. et al. Plasticity of functional traits varies clinally along a rainfall gradient inEucalyptus tricarpa. *Plant Cell Environ.* **37**, 1440–1451 (2014).
45. Oyanoghafo, O. O. et al. Contributions of phenotypic integration, plasticity and genetic adaptation to adaptive capacity relating to drought in *Banksia marginata* (Proteaceae). *Front. Plant Sci.* **14**, 1150116 (2023).
46. Vivas, M., Rolo, V., Wingfield, M. J. & Slippers, B. Maternal environment regulates morphological and physiological traits in *Eucalyptus grandis*. *For. Ecol. Manage.* **432**, 631–636 (2019).
47. Ramírez-Valiente, J. A. et al. Limited plastic responses in safety traits support greater hydraulic risk under drier conditions. *Nat. Ecol. Evol.* **9**, 1825–1836 (2025).
48. Zanne, A. E. et al. Three keys to the radiation of angiosperms into freezing environments. *Nature* **506**, 89–92 (2014).
49. Muscarella, R. et al. Variation of tropical forest assembly processes across regional environmental gradients. *Perspect. Plant Ecol. Evol. Syst.* **23**, 52–62 (2016).

Methods

Study site and species selection

Puerto Rico spans 8,740 km^2 and encompasses six Holdridge life zones. The MAP ranges from 800 mm in subtropical dry forests to more than 4,000 mm in subtropical rainforests[28,50]. The primary soil types are derived from limestone and volcanic parent materials[29,51,52]. Limestone soils, which have lower water-holding capacity and nutrients, are generally found in drier regions, and the volcanic soils, with higher water-holding capacity, occur in wetter areas[28,30,49]. We selected six forest reserves distributed across the island spanning a MAP from around 1,000 to 4,000 mm. Three of the study sites are located on limestone soils and three on volcanic soils (Fig. 1 and Extended Data Table 1). On the basis of previous ecological studies at these sites, we identified tree species that occurred in at least two sites[31,49], and measured hydraulic traits (see below) for each species at all sites where it was present, ranging from two to four sites per species (Extended Data Table 2).

Environmental data

MAP was derived from the Parameter-elevation Regressions on Independent Slopes Model (PRISM Climate Group, Oregon State University, https://prism.oregonstate.edu, accessed 25 April 2023). Geological substrate (soil parent material) data were obtained from ref. 30.

Hydraulic traits

We collected two >1.5 m long canopy branches with a pole pruner from each individual tree. We sealed the branches in large black plastic bags with wet paper towels and transported them out of the forest. Once we reached our vehicle, we placed the branches in large plastic garbage cans with water, recut the branches under water, and kept them covered with the black plastic bags to minimize evapotranspiration while we transported them to the laboratory. All branches were collected in the morning between 07:00 and 09:00 a.m. local time. At the end of each collecting trip, we immediately took the samples to the laboratory where we conducted the hydraulic measurements. Depending on the distance from the site to the laboratory, this period was between 1 and 2 h. If we had to repeat any of the measurements, we would collect more branches from the same individual tree sampled before. The bulk of the hydraulic trait measurements were conducted between July 2019 and June 2021, with one final campaign in June 2023. Owing to the logistical challenges of transporting branches back to a laboratory within 2 h of collection, we first worked out of two laboratories on the north side of the island, where we sampled El Yunque 300–400 m, El Yunque 500–600 m and Cambalache. We then moved to a laboratory on the west side of the island to sample Guajataca, Guilarte and Guanica. We avoided sampling the drier sites, namely Cambalache, Guajataca and Guanica, during the peak of the dry season in March and April, so that all sites were sampled during the wet season (>100 mm of mean monthly precipitation). Although sites were sampled during the wet season, rainfall variability might have affected the hydraulic traits that potentially can adjust throughout the year, such as TLP[53].

Leaf and stem PV curves

We measured leaf TLP, leaf and stem SWC and water storage capacity of leaves and stems using pressure–volume (PV) curves. For the PV curves, we used the bench dry method described previously[54]. For the leaf PV curves, we let the branch rehydrate overnight, then, using a razor blade, excised a mature fully expanded healthy leaf from the branch and sealed it in a Whirl-Pak bag. As the leaf dried, we periodically measured water potential (Ψ) with a pressure chamber instrument (PMS Instruments) and leaf weight (3-decimal-point balance, OHAUS Scout). We continued to measure the leaf until the relationship between $1/\Psi$ and water loss became linear. Lastly, we dried the leaf in an oven at 65 °C for more than 72 h and weighed it to obtain the leaf dry mass. We constructed the PV curves used the ref. 55 spreadsheet tool, from which we extracted the leaf TLP, leaf SWC, leaf CFT and leaf CTLP.

For the stem PV curves, we excised approximately 1–1.5-m-long intact terminal branches immediately after the samples were brought back from the field, removed all the leaves from the branch, and wrapped Parafilm (Bemis) around any cuts in the bark to seal them. We attached a stem psychrometer (ICT International) to the branch by removing a small section of bark from the branch, washing the exposed xylem with deionized water, drying it with Kimwipes (Kimberly-Clark), clamping the psychrometer to the exposed xylem and creating an air-tight seal with Parafilm. We set the psychrometers to record water potential every 10 min. As the branch dried, we periodically weighed it (2-decimal-point balance, OHAUS Scout). We continued to log water potential and branch weight until $1/\Psi$ and water loss became linear. Lastly, we dried the branch in an oven at 65 °C for 1 week and weighed it to obtain the branch dry mass. The same as with the leaves, we used a previously described tool[55] to construct the branch PV curves, from which we extracted the stem SWC, stem CFT and stem CTLP. We could not do stem PV curves for the palm, *Prestoea acuminata* var. *montana*, owing to its monocot anatomy.

Leaf and stem OV curves

We used the optical vulnerability (OV) technique to estimate xylem embolism accumulation in leaves and stems following refs. 56,57. For each branch, we clamped one leaf and a small distal stem (around 3–6 mm in diameter depending on the species) inside a custom-built clamp (OpenSourceOV, OSOV) with an 8-megapixel Raspberry Pi camera and 6 light-emitting diodes operated by a Raspberry Pi microcomputer. Further details for OSOV clamps construction, image capturing and post-image processing can be found online (http://www.opensourceov.org). In brief, for the leaves, we selected a healthy, fully expanded leaf, placed a microscope slide over the area to be imaged and clamped it onto the OSOV clamp. For stems, we removed a small area of bark (around 2 cm^2) from a distal stem with healthy foliage to expose the xylem. We applied adhesive hydrogel (Tensive) to the exposed xylem to reduce surface reflection, help light penetration into the xylem and reduce desiccation. We covered the hydrogel with a round-glass coverslip and clamped it in the OSOV clamp. We set the OSOV clamps to take a picture every 5 min until no embolism events were recorded for at least 12 h (around 72–96 h depending on the species). We used stem psychrometers to measure water potential every 10 min as the branches dried. We were unable to obtain OV data for stems of *Cecropia schreberiana* and the palm, *P. acuminata* var. *montana*, owing to their anatomy. We chose to use the OV technique over other techniques for measuring xylem vulnerability to embolism, as it has been validated in many studies for many species and can be used simultaneously on leaves and stems[56–64].

We used ImageJ software (v.1.54p; National Institutes of Health) to process all the pictures of leaf and stem to extract embolisms following refs. 56,57. In brief, we stacked all the pictures in chronological order and converted them to 8-bit greyscale with pixel values ranging from black (0) to white (255). Each picture was subtracted from the next picture in the sequence to reveal embolisms, which appear in the image differences as changes in light intensity (differences in pixel values). We removed all the differences in pixels that were due to noise or artefacts (for example, sample movements or shrinkage) using both the remove outlier function in ImageJ and manually, leaving only the differences in pixels belonging to embolisms. The accumulation of embolisms in each leaf and stem was quantified as a cumulative total of embolized pixels in each picture divided by the total number of embolized pixels in the full stack of pictures from the dried sample. To estimate the water potential at the time of each picture capture (Ψ_x), we fitted a linear regression to the water potential measurements over time. With this, we created the vulnerability curves and extracted the values at which 50% of the cumulative embolism had occurred (P_{50}). We calculated P_{50}

for both leaves (leaf P_{50}) and stems (stem P_{50}). The complete details of the methods for the OV curves, including an overview of the technique, instructions for image processing, as well as ImageJ scripts, are available online (http://www.opensourceov.org). We calculated stomatal safety margins as leaf TLP − P_{50}. We chose to use P_{50} instead of Ψ_x at 88% of the cumulative embolism P_{88} because, in a previous study, we found that P_{88} exhibits substantially higher within-individual variability than P_{50} (ref. 65).

Data analysis

To assess shifts between drought avoidance and drought tolerance strategies across the rainfall gradient, we fitted linear regression models for each of the 11 hydraulic traits using species-level mean trait values per site as the response variable and MAP as the predictor. We recognize that leaf phenology is one axis of variation in drought avoidance and sampled all leaves for the two drought-deciduous species when they were fully leafed out. We examined how good a prediction we could obtain without the two drought-deciduous species, but as it did not change model fits, we did not consider this trait in the final analyses.

To evaluate species-level trait response to MAP across the different sites where each species was measured, we fitted separate mixed effects models for each species and trait combination, using trait values from all the individual trees with hydraulic traits as the response variables, MAP as the fixed effect, and site as a random intercept. Models were fitted using the lme4 (ref. 66) and lmerTest[67] packages. Using all the individual trait measurements allowed us to retain within-site variation, as no averaging was performed at the species by site level, while including site as a random intercept captured site level variation not accounted by MAP and avoided pseudoreplication.

To quantify the extent to which variation in hydraulic traits was driven by species turnover versus intraspecific variation across sites, we fitted a series of Bayesian hierarchical models (one for each hydraulic trait) using the brms package[68]. For all the models, we used weakly informative normal priors, four Markov chain Monte Carlo chains with 4,000 total iterations and 50% of them as warmup iterations. Models were based on individual-level tree data for all traits and included as response variables hydraulic traits associated with drought tolerance (leaf P_{50}, stem P_{50}, leaf SMP_{50}, stem SMP_{50} and Ψ_{TLP}) and those associated with drought avoidance (leaf SWC, leaf CFT, leaf CTLP, stem SWC, stem CFT and stem CTLP). All models included MAP as a fixed effect, but the four models differed in the inclusion and structure of the random effects. The first model (the baseline model) included only MAP, assuming no differences among species in average hydraulic trait values or responses to rainfall. The second model included only random intercepts for species, capturing variation across sites that can be attributed to species turnover, but assuming a uniform response to precipitation for all species. The third model included only random slopes to account for the fact that the association between drought strategies and MAP is also likely to vary by species (intraspecific variation) but no additional effect of species. Finally, the fourth model included both random intercepts and slopes, which accounts for species turnover and differences among species in their response to precipitation. We then calculated conditional R^2 (fixed + random effects), marginal R^2 (only the fixed effect of rainfall) and LOO elpd (leave-one-out cross-validation expected log posterior density) for each model. Higher LOO elpd values indicate a better fit of the model. Based on LOO elpd, we calculated elpd difference and LOO elpd standard error difference among models to determine the best model. A higher LOO elpd and conditional R^2 for the fourth model relative to the model that includes only random intercepts (that is, species turnover) and a fixed effect of rainfall indicate that intraspecific variation in hydraulic traits is a significant factor in structuring forest drought resistance. In other words, if the full mixed-effects model, which includes both species-level intercepts and species-specific trait–rainfall slopes, has the highest LOO elpd and conditional R^2, this indicates that allowing species to differ in their trait–environment responses (that is, intraspecific variation) substantially improves model performance. In all of the models, we scaled MAP to standardize the values and facilitate convergence. Using the insight package[69], we extracted the proportion of variance explained by slopes (intraspecific trait variation), intercepts (species turnover), fixed effect (MAP) and the residual unexplained variance from the fourth model, which included both random intercepts and slopes. We performed all analyses using R statistical software (R v.4.4.2). All data used for the analyses and the R code are available at Dryad (https://doi.org/10.5061/dryad.r4xgxd2vb)[70].

Reporting summary

Further information on research design is available in the Nature Portfolio Reporting Summary linked to this article.

Data availability

All data have been deposited to the Dryad digital repository[70] (https://doi.org/10.5061/dryad.r4xgxd2vb).

Code availability

All R code has been deposited to the Dryad digital repository[70] (https://doi.org/10.5061/dryad.r4xgxd2vb).

50. Ewel, J. J. & Whitmore, J. L. *The Ecological Life Zones of Puerto Rico and the U.S. Virgin Islands* (Institute of Tropical Forestry, 1973).
51. Lugo-Camacho, J. L. *The Soil Climate Regimes of Puerto Rico: Reassessment and Implications*. MSc thesis, Univ. of Puerto Rico (2005).
52. Sanchez, M. J., Lopez, E. & Lugo, A. E. *Chemical and Physical Analyses of Selected Plants and Soils from Puerto Rico (1981-2000)* (US Department of Agriculture, 2015).
53. Maréchaux, I., Bartlett, M. K., Iribar, A., Sack, L. & Chave, J. Stronger seasonal adjustment in leaf turgor loss point in lianas than trees in an Amazonian forest. *Biol. Lett.* **13**, 20160819 (2017).
54. Tyree, M. T. & Hammel, H. T. The measurement of the turgor pressure and the water relations of plants by the pressure-bomb technique. *J. Exp. Bot.* **23**, 267–282 (1972).
55. Sack, L. & Pasquet-Kok, J. Leaf pressure–volume curve parameters. *Prometheus* https://prometheusprotocols.net/function/water-relations/pressure-volume-curves/leaf-pressure-volume-curve-parameters/ (2011).
56. Brodribb, T. J. et al. Visual quantification of embolism reveals leaf vulnerability to hydraulic failure. *N. Phytol.* **209**, 1403–1409 (2016).
57. Brodribb, T. J., Carriqui, M., Delzon, S. & Lucani, C. Optical measurement of stem xylem vulnerability. *Plant Physiol.* **174**, 2054–2061 (2017).
58. Smith-Martin, C. M., Skelton, R. P., Johnson, K. M., Lucani, C. & Brodribb, T. J. Lack of vulnerability segmentation among woody species in a diverse dry sclerophyll woodland community. *Funct. Ecol.* **34**, 777–787 (2020).
59. Skelton, R. P. et al. Low vulnerability to xylem embolism in leaves and stems of North American oaks. *Plant Physiol.* **177**, 1066–1077 (2018).
60. Brodribb, T. J., Carriquí, M., Delzon, S., McAdam, S. A. M. & Holbrook, N. M. Advanced vascular function discovered in a widespread moss. *Nat. Plants* **6**, 273–279 (2020).
61. Gauthey, A. et al. Visual and hydraulic techniques produce similar estimates of cavitation resistance in woody species. *N. Phytol.* **228**, 884–897 (2020).
62. Johnson, K. M., Brodersen, C., Carins-Murphy, M. R., Choat, B. & Brodribb, T. J. Xylem embolism spreads by single-conduit events in three dry forest angiosperm stems. *Plant Physiol.* **184**, 212–222 (2020).
63. Pereira, L. et al. The Pneumatron: an automated pneumatic apparatus for estimating xylem vulnerability to embolism at high temporal resolution. *Plant Cell Environ.* **43**, 131–142 (2020).
64. Guan, X., Pereira, L., McAdam, S. A. M., Cao, K. F. & Jansen, S. No gas source, no problem: proximity to pre-existing embolism and segmentation affect embolism spreading in angiosperm xylem by gas diffusion. *Plant Cell Environ.* **44**, 1329–1345 (2021).
65. Smith-Martin, C. M. et al. Increasing air-filled vessels has little influence on vulnerability to drought-induced embolism in two species with long maximum xylem vessel length but low vessel connectivity. *Tree Physiol.* **45**, tpaf041 (2025).
66. Bates, D., Mächler, M., Bolker, B. & Walker, S. Fitting linear mixed-effects models using lme4. *J. Stat. Softw.* **67**, 1–48 (2015).
67. Kuznetsova, A., Brockhoff, P. B. & Christensen, R. H. B. lmerTest package: tests in linear mixed effects models. *J. Stat. Softw.* **82**, 1–26 (2017).
68. Bürkner, P.-C. brms: an R package for bayesian multilevel models using Stan. *J. Stat. Softw.* **80**, 1–28 (2017).
69. Lüdecke, D., Waggoner, P. & Makowski, D. insight: a unified interface to access information from model objects in R. *J. Open Source Softw.* **4**, 1412 (2019).
70. Smith-Martin, C. M., Muscarella, R., Brodribb, T. J. & Uriarte, M. Data and code for 'Species intraspecific variation drives tropical forest drought resistance'. *Dryad* https://doi.org/10.5061/dryad.r4xgxd2vb (2026).

71. PRISM Group. *PRISM Database* (2014, accessed 14 November 2025); https://prism.oregonstate.edu.
72. Karger, D. N. et al. Climatologies at high resolution for the earth's land surface areas. *Sci. Data* **4**, 170122 (2017).
73. Little, A. L. & Wadsworth, F. H. *Common Trees of Puerto Rico and the Virgin Islands* Agriculture Handbook No. 249 (US Department of Agriculture, 1964).

Acknowledgements We thank S. L. Farrar, M. Salva-Sauri, O. Geli and C. Hale, who helped collect the hydraulic trait data; and B. van Ee granted us access to his laboratory.

Author contributions C.M.S.-M., R.M. and M.U. conceived the study. C.M.S.-M. and M.U. collected the data. C.M.S.-M., R.M. and M.U. performed the analyses. C.M.S.-M. and M.U. wrote the manuscript with input from T.J.B. and R.M.

Funding This work was supported by US National Science Foundation (NSF) DEB-1753810 to M.U. and R.M. and the Australian Research Council Centre of Excellence for Plant Success in Nature and Agriculture: CE170100009 to T.J.B.

Competing interests The authors declare no competing interests.

Additional information

Supplementary information The online version contains supplementary material available at https://doi.org/10.1038/s41586-026-10870-4.

Correspondence and requests for materials should be addressed to Chris M. Smith-Martin.

Peer review information *Nature* thanks Brendan Choat, Jordi Martínez-Vilalta and the other, anonymous, reviewer(s) for their contribution to the peer review of this work. Peer reviewer reports are available.

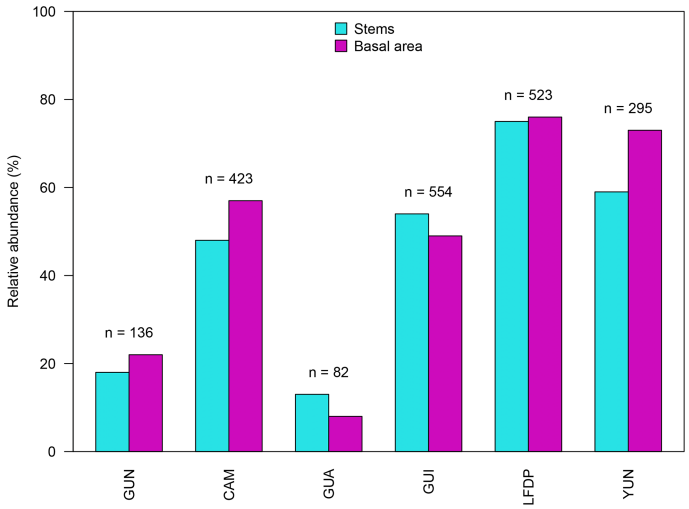

Extended Data Fig. 1 | Relative abundance (based on counts of individual stems and basal area of all trees with a diameter at breast height ≥ 5 cm) of species sampled for hydraulic traits in six plots.

Extended Data Table 1 | Characteristics of the six sites where we conducted the hydraulic measurements (MAP = mean annual precipitation, Tmax = maximum monthly temperature, VPD = vapour pressure deficit)

Site	Site Code	Soil type	MAP (mm yr^{-1})	Tmax (°C)	VPD (Pa)	Stem density (ha^{-1})	Mean canopy height (m)
Guanica	GUN	Limestone	1,004	30.5	1,290	5,856	6.8
Cambalache	CAM	Limestone	1,386	30.7	1,356	3,872	15.5
Guajataca	GUA	Limestone	2,017	29.1	1,110	3,138	21.2
Guilarte	GUI	Volcanic	2,195	25.6	912	2,454	18.5
El Yunque 300-400 m	LFDP	Volcanic	3,593	26.8	920	2,118	19.8
El Yunque 500-600 m	YUN	Volcanic	4,029	25.5	783	2,618	17.1

MAP and Tmax data are extracted from PRISM[71]; VPD is extracted from Chelsa Climate data[72]; Stem density per ha is based on the trees ≥2.5 cm DBH[49]. Mean canopy height is based on airborne lidar data from the plots[36].

Extended Data Table 2 | List of the species measured, their families, species codes, leaf phenology (evergreen and drought-deciduous), sites where each species was measured, species-level maximum height[73], and relative basal area for the species in each given site

Species	Family	Phenology	Sites Code	Max height (m)
Alchornea latifolia	Euphorbiaceae	evergreen	GUI	15
Alchornea latifolia	Euphorbiaceae	evergreen	YUN	15
Alchornea latifolia	Euphorbiaceae	evergreen	LFDP	15
Bursera simaruba	Burseraceae	deciduous	CAM	12
Bursera simaruba	Burseraceae	deciduous	GUA	12
Bursera simaruba	Burseraceae	deciduous	GUN	12
Casearia arborea	Flacourtiaceae	evergreen	GUI	9
Casearia arborea	Flacourtiaceae	evergreen	YUN	9
Casearia arborea	Flacourtiaceae	evergreen	LFDP	9
Cecropia schreberiana	Moraceae	evergreen	GUI	21
Cecropia schreberiana	Moraceae	evergreen	YUN	21
Cecropia schreberiana	Moraceae	evergreen	LFDP	21
Coccoloba diversifolia	Polygonaceae	evergreen	CAM	9
Coccoloba diversifolia	Polygonaceae	evergreen	GUN	9
Dacryodes excelsa	Burseraceae	evergreen	GUI	30
Dacryodes excelsa	Burseraceae	evergreen	YUN	30
Dacryodes excelsa	Burseraceae	evergreen	LFDP	30
Drypetes glauca	Euphorbiaceae	evergreen	GUI	9
Drypetes glauca	Euphorbiaceae	evergreen	YUN	9
Drypetes glauca	Euphorbiaceae	evergreen	LFDP	9
Erythroxylum rotundifolium	Erythroxylaceae	evergreen	CAM	6
Erythroxylum rotundifolium	Erythroxylaceae	evergreen	GUN	6
Faramea occidentalis	Rubiaceae	evergreen	CAM	9
Faramea occidentalis	Rubiaceae	evergreen	GUA	9
Guarea guidonia	Meliaceae	evergreen	GUI	23
Guarea guidonia	Meliaceae	evergreen	LFDP	23
Inga laurina	Fabaceae	evergreen	GUI	21
Inga laurina	Fabaceae	evergreen	YUN	21
Inga laurina	Fabaceae	evergreen	LFDP	21
Krugiodendron ferreum	Rhamnaceae	evergreen	CAM	5
Krugiodendron ferreum	Rhamnaceae	evergreen	GUN	5
Micropholis guyanensis	Sapotaceae	evergreen	GUI	15
Micropholis guyanensis	Sapotaceae	evergreen	YUN	15
Micropholis guyanensis	Sapotaceae	evergreen	LFDP	15
Ocotea leucoxylon	Lauraceae	evergreen	GUA	15
Ocotea leucoxylon	Lauraceae	evergreen	GUI	15
Ocotea leucoxylon	Lauraceae	evergreen	YUN	15
Ocotea leucoxylon	Lauraceae	evergreen	LFDP	15
Poitea florida	Fabaceae	deciduous	CAM	15
Poitea florida	Fabaceae	deciduous	GUN	15
Prestoea acuminata var. montana	Arecaceae	evergreen	GUI	23
Prestoea acuminata var. montana	Arecaceae	evergreen	YUN	23
Prestoea acuminata var. montana	Arecaceae	evergreen	LFDP	23
Sloanea berteroana	Elaeocarpaceae	evergreen	GUI	28
Sloanea berteroana	Elaeocarpaceae	evergreen	YUN	28
Sloanea berteroana	Elaeocarpaceae	evergreen	LFDP	28
Tabebuia heterophylla	Bignonaceae	evergreen	GUA	18
Tabebuia heterophylla	Bignonaceae	evergreen	GUN	18
Tabebuia heterophylla	Bignonaceae	evergreen	YUN	18
Tabebuia heterophylla	Bignonaceae	evergreen	LFDP	18

nature portfolio

Corresponding author(s): Chris Smith-Martin

Last updated by author(s): Jun 20, 2026

Reporting Summary

Nature Portfolio wishes to improve the reproducibility of the work that we publish. This form provides structure for consistency and transparency in reporting. For further information on Nature Portfolio policies, see our Editorial Policies and the Editorial Policy Checklist.

Statistics

For all statistical analyses, confirm that the following items are present in the figure legend, table legend, main text, or Methods section.

n/a	Confirmed	
☐	☒	The exact sample size (*n*) for each experimental group/condition, given as a discrete number and unit of measurement
☐	☒	A statement on whether measurements were taken from distinct samples or whether the same sample was measured repeatedly
☐	☒	The statistical test(s) used AND whether they are one- or two-sided *Only common tests should be described solely by name; describe more complex techniques in the Methods section.*
☐	☒	A description of all covariates tested
☐	☒	A description of any assumptions or corrections, such as tests of normality and adjustment for multiple comparisons
☐	☒	A full description of the statistical parameters including central tendency (e.g. means) or other basic estimates (e.g. regression coefficient) AND variation (e.g. standard deviation) or associated estimates of uncertainty (e.g. confidence intervals)
☐	☒	For null hypothesis testing, the test statistic (e.g. *F*, *t*, *r*) with confidence intervals, effect sizes, degrees of freedom and *P* value noted *Give P values as exact values whenever suitable.*
☐	☒	For Bayesian analysis, information on the choice of priors and Markov chain Monte Carlo settings
☐	☒	For hierarchical and complex designs, identification of the appropriate level for tests and full reporting of outcomes
☒	☐	Estimates of effect sizes (e.g. Cohen's *d*, Pearson's *r*), indicating how they were calculated

Our web collection on statistics for biologists contains articles on many of the points above.

Software and code

Policy information about availability of computer code

Data collection

For the leaf and stem optical vulnerability curves, we used the optical vulnerability technique using costume made Cavicams as described by Brodribb et al. (2016) , Brodribb et al. (2017) and at https://www.opensourceov.org/. We used ImageJ software (Version 1.54p; National Institutes of Health, USA) to analyze the pictures of leaf and stem embolisms. For the pressure volume curves we used the bench dehydration method as decried by Tyree & Hammel (1972) and Sack & Pasquet-Kok (2011).

References:
Brodribb, T. J., M. Carriqui, S. Delzon, and C. Lucani. 2017. Optical Measurement of Stem Xylem Vulnerability. Plant Physiology 174:2054-2061.
Brodribb, T. J., R. P. Skelton, S. A. M. McAdam, D. Bienaimé, C. J. Lucani, and P. Marmottant. 2016. Visual quantification of embolism reveals leaf vulnerability to hydraulic failure. New Phytologist 209:1403-1409.
Sack, L. & Pasquet-Kok, J. Leaf pressure–volume curve parameters. (2011).
Tyree, M. T. & Hammel, H. T. The Measurement of the Turgor Pressure and the Water Relations of Plants by the Pressure-bomb Technique. Journal of Experimental Botany 23, 267-282 (1972).

Data analysis

We performed all statistical analyses using R statistical software version R 4.4.2. The mixed effects models fitted using the lme4 (Bates et al. 2015) and lmerTest (Kuznetsova et al. 2017) packages. To fit the Bayesian hierarchical models, we used the brms package (Bürkner 2017) and the insight package (Lüdecke et al. 2019).

References:
Bates, D., Mächler, M., Bolker, B. & Walker, S. Fitting Linear Mixed-Effects Models Using lme4. Journal of Statistical Software 67, 1 - 48 (2015).
Bürkner, P.-C. 2017. brms: An R Package for Bayesian Multilevel Models Using Stan. Journal of Statistical Software 80:1 - 28.

Lüdecke, D., P. Waggoner, and D. Makowski. 2019. insight: A Unified Interface to Access Information from Model Objects in R. Journal of Open Source Software 4:1412.
Kuznetsova, A., P. B. Brockhoff, and R. H. B. Christensen. 2017. lmerTest Package: Tests in Linear Mixed Effects Models. Journal of Statistical Software 82:1 - 26.

For manuscripts utilizing custom algorithms or software that are central to the research but not yet described in published literature, software must be made available to editors and reviewers. We strongly encourage code deposition in a community repository (e.g. GitHub). See the Nature Portfolio guidelines for submitting code & software for further information.

Data

Policy information about availability of data

All manuscripts must include a data availability statement. This statement should provide the following information, where applicable:

- Accession codes, unique identifiers, or web links for publicly available datasets
- A description of any restrictions on data availability
- For clinical datasets or third party data, please ensure that the statement adheres to our policy

All data used for the analyses and the R code are available here DOI: 10.5061/dryad.r4xgxd2vb. There is one CSV with all hydraulic trait data and mean annual precipitation that was derived from Parameter-elevation Regressions on Independent Slopes Model (PRISM Climate Group, Oregon State University, https://prism.oregonstate.edu, accessed 25 April 2023).

Research involving human participants, their data, or biological material

Policy information about studies with human participants or human data. See also policy information about sex, gender (identity/presentation), and sexual orientation and race, ethnicity and racism.

Reporting on sex and gender	N/A
Reporting on race, ethnicity, or other socially relevant groupings	N/A
Population characteristics	N/A
Recruitment	N/A
Ethics oversight	N/A

Note that full information on the approval of the study protocol must also be provided in the manuscript.

Field-specific reporting

Please select the one below that is the best fit for your research. If you are not sure, read the appropriate sections before making your selection.

☐ Life sciences ☐ Behavioural & social sciences ☒ Ecological, evolutionary & environmental sciences

For a reference copy of the document with all sections, see nature.com/documents/nr-reporting-summary-flat.pdf

Ecological, evolutionary & environmental sciences study design

All studies must disclose on these points even when the disclosure is negative.

Study description	We measured 11 plant hydraulic traits for 18 tree species in six different forest reserves spanning the island's rainfall gradient (Fig. 1 and Extended Data Table 1; 2). These included traits linked to drought avoidance—leaf and stem capacitance (C), saturated water content (SWC)—and drought tolerance—leaf and stem xylem vulnerability to embolisms (P50) and stomatal safety margins (SM).
Research sample	Based on previous ecological studies at these six sites, we identified abundant tree species that occurred at multiple of these sites (Muscarella et al. 2016, Muscarella et al. 2020). We identified 18 abundant species that occurred at multiple of the six sites. Traits were measured on as many of the 18 species that occurred at each of the six sites, totaling 290 trees, with all species measured at two to four locations. References: Muscarella, R., S. Kolyaie, D. C. Morton, J. K. Zimmerman, and M. Uriarte. 2020. Effects of topography on tropical forest structure depend on climate context. JOURNAL OF ECOLOGY 108:145-159. Muscarella, R., M. Uriarte, D. L. Erickson, N. G. Swenson, W. J. Kress, and J. K. Zimmerman. 2016. Variation of tropical forest assembly processes across regional environmental gradients. Perspectives in Plant Ecology, Evolution and Systematics 23:52-62.

Sampling strategy	At each site, we measured leaf and stem pressure-volume curves and leaf and stem optical vulnerability curves on average on five trees of each species of the 18 species at each of the sites where that occurred (ED Table 3).
Data collection	We measured leaf and stem pressure-volume curves using the bench dry method described by Tyree and Hammel (1972). For leaves, we let the branch rehydrate overnight, excised a mature fully expanded healthy leaf from the branch with a sharp razor blade, and immediately sealed it in a Whirl-Pak bag (Whirl-Pak, Madison, WI, USA). As leaves dehydrated, we periodically measured water potential (Ψ) with a Pressure Chamber Instrument (PMS Instrument Company, Albany, OR, USA) and leaf weight on a balance. We entered all the data as it was collected in Google spreadsheets. For stems, we excised ~1–1.5 m long intact terminal branches immediately after the samples were brought back from the field, removed all the leaves, and sealed any cuts in the bark with Parafilm (Parafilm sealing film, Bemis Company, Neenah, WI, USA). As the branch dehydrated, we used a stem psychrometer (ICT International, Armidale, Australia) to record water potential every 10 min and periodically weighed the branch with a balance. We entered the data into a Google spreadsheet and uploaded to Google Drive each of the data file outputs from the stem psychrometer data loggers. We used the optical vulnerability (OV) technique to estimate xylem embolism accumulation in leaves and stems as described by Brodribb et al. (2016) and Brodribb et al. (2017). Briefly, for each branch immediately after it was brought back from the field, we secured a leaf and a small distal stem (~ 3–6 mm in diameter depending on the species) inside a custom-built three-dimensional printed clamp (OpenSourceOV, OSOV) fitted with a small 8-megapixel Raspberry Pi camera and six bright light-emitting diodes operated by a Raspberry Pi microcomputer. While the branches were drying, we used stem psychrometers to measure water potential every 10 minutes. We uploaded to Google Drive all the photos and the data files from the stem psychrometers. References: Brodribb, T. J., M. Carriqui, S. Delzon, and C. Lucani. 2017. Optical Measurement of Stem Xylem Vulnerability. Plant Physiology 174:2054-2061. Brodribb, T. J., R. P. Skelton, S. A. M. McAdam, D. Bienaimé, C. J. Lucani, and P. Marmottant. 2016. Visual quantification of embolism reveals leaf vulnerability to hydraulic failure. New Phytologist 209:1403-1409. Tyree, M. T., and H. T. Hammel. 1972. The Measurement of the Turgor Pressure and the Water Relations of Plants by the Pressure-bomb Technique. Journal of Experimental Botany 23:267-282.
Timing and spatial scale	All hydraulic measurements were conducted between July 2019 and June 2023. We did continues sampling from July 2019 and June 2022 and then a final sampling during June 2023.
Data exclusions	No data was excluded from the sampling.
Reproducibility	All details are described in the Methods section on how we selected the species, collected the leaf and stem pressure-volume curves, and the leaf and stem optical vulnerability curves. We measured on average 5 trees of each species at each site, and we have added these details in the Extended data (ED Table 3).
Randomization	Randomization was not relevant to our study as we were targeting specific species at each of the six study sites across the rainfall gradient.
Blinding	Blinding was not relevant to our study.

Did the study involve field work? ☒ Yes ☐ No

Field work, collection and transport

Field conditions	The study was conducted in six locations across the Caribbean Island of Puerto Rico spans 8,740 km2 and encompasses six Holdridge life zones. Mean annual precipitation ranges from 800 mm in subtropical dry forests to over 4,000 mm in subtropical rainforests. The primary soil types are derived from limestone and volcanic parent materials. Limestone soils, which have lower water-holding capacity and nutrients, are generally found in drier regions and the volcanic soils with higher water-holding capacity, occur in wetter areas.
Location	We selected six forest reserves distributed across the island, spanning a mean annual precipitation (MAP) from ca. 1,000 to 4,0000 mm. Six sites with their soil parent material, rainfall and coordinates: Guanica, limestone 1,004 mm, 17°58'25.1"N 66°51'15.9"W Cambalache, limestone, 1,386 mm, 18°26'51.1"N 66°35'38.3"W Guajataca, limestone, 2,017 mm, 18°21'55.2"N 66°58'14.6"W Guilarte , volcanic, 2,195 mm, 18°06'33.4"N 66°44'49.8"W El Yunque 300-400 m, volcanic, 3,593 mm, 18°19'12.0"N 65°48'36.0"W El Yunque 500-600 m, volcanic, 4,029 mm,18°19'18.1"N 65°48'11.8"W
Access & import/export	We worked under the umbrella of the Luquillo Long-Term Ecological Research Site.
Disturbance	Our sampling did not cause significant disturbances to the plot. Sun exposed terminal branches were collected using pole pruners.

Reporting for specific materials, systems and methods

We require information from authors about some types of materials, experimental systems and methods used in many studies. Here, indicate whether each material, system or method listed is relevant to your study. If you are not sure if a list item applies to your research, read the appropriate section before selecting a response.

Materials & experimental systems

n/a	Involved in the study
☒	☐ Antibodies
☒	☐ Eukaryotic cell lines
☒	☐ Palaeontology and archaeology
☒	☐ Animals and other organisms
☒	☐ Clinical data
☒	☐ Dual use research of concern
☒	☐ Plants

Methods

n/a	Involved in the study
☒	☐ ChIP-seq
☒	☐ Flow cytometry
☒	☐ MRI-based neuroimaging

Plants

Seed stocks	We worked with native tree species in Puerto Rico, so this does not apply.
Novel plant genotypes	We worked with native tree species in Puerto Rico, so this does not apply.
Authentication	We worked with native tree species in Puerto Rico, so this does not apply.